In The Physics of Magnetic Flux Ropes, Proc. Sydney Chapman Conference in Bermuda, March 1989.

1990:

WAVES IN SOLAR PHOTOSPHERIC FLUX TUBES AND THEIR INFLUENCE ON THE OBSERVABLE SPECTRUM

S.K. Solanki and B. Roberts

The Mathematical Institute, University of St. Andrews, St. Andrews, KY16 9SS, Scotland

Abstract: Linear calculations of undamped magnetoacoustic waves in thin solar magnetic flux tubes are presented and their influence on the Stokes V profiles of various iron lines is studied. This is a necessary first step for the diagnostics of the properties of flux tube waves, in particular the amount of energy transported by them into the upper atmosphere. It is shown that, with sufficiently high spatial resolution, observations can distinguish between standing and propagating waves on the basis of line parameters of photospheric spectral lines alone. Particular attention is given to exploring quantitative diagnostics for the wave amplitude, since it is currently the most important unknown parameter determining the energy flux carried by the waves. It is found that although this parameter can be derived relatively simply if the thermal fluctuations produced by the wave are ignored (i.e. for an isothermal wave), the task becomes much more complex for the more realistic case of a coupled variation of temperature and velocity.

1. Introduction

Physical considerations lead us to expect a rich variety of wave modes in solar magnetic flux tubes, including longitudinal tube waves (cf. Spruit and Roberts, 1983; Roberts, 1984, 1986; Thomas, 1985). Indirect observational evidence for the presence of large amplitude longitudinal waves in solar flux tubes is also mounting (Solanki, 1986, 1989), although direct evidence is still lacking. Such waves are expected to play an important role in heating the outer solar atmosphere. So far investigations of waves in flux tubes have either concentrated on the purely MHD aspects, which have been dealt with in great detail by various authors (e.g., Defouw, 1976; Roberts and Webb, 1978, 1979; Webb and Roberts, 1980; Spruit, 1981; Rae and Roberts, 1982; Herbold et al., 1985; Musielak et al., 1989), or on the purely observational. No attempts have been made to combine the two approaches quantitatively. Indeed, we have only a rough qualitative idea of what the observational signatures of flux tube waves are. Here, we describe the first investigation of the influence of longitudinal flux tube waves on spectral line profiles, in particular on Stokes V profiles which are the main carriers of information on magnetic elements or small flux tubes. We hope to identify the observations best suited to deriving information on flux tube waves, and to develop methods for their analysis. In a future step presently available observations may also be used to diagnose some interesting parameters, e.g. to set limits on the energy flux being carried by such waves into the chromosphere. We do not attempt to reproduce directly the observations at this stage.

2. Longitudinal Flux Tube Waves

2.1. Summary of Hydrodynamics

The basic assumptions of the model are: 1) The flux tube structure is described by the thin tube approximation (Defouw, 1976; Roberts and Webb, 1978, 1979; Parker, 1979), which agrees very well with observations (Zayer et al., 1989). 2) The waves considered are linear. This assumption allows us to vary wave parameters easily, thus permitting us to assess the influence of waves over as wide a range of properties as possible. 3) Radiative damping is neglected. Its influence will be studied in a future publication. 4) The gas inside the flux tube is not coupled to the field free surroundings; i.e. the calculated flux tube waves do not excite

disturbances in the field-free atmosphere surrounding the flux tube.

For the calculation of the flux tube wave the following differential equation for the normalized velocity, Q, must be solved (see Roberts and Webb, 1978, for a derivation):

$$\frac{\mathrm{d}^2 Q}{\mathrm{d}z^2} + \left(\frac{\omega^2 - \Omega^2(z)}{c_T^2} \right) Q = 0; \tag{1}$$

$Q(z)$ is related to the local longitudinal velocity, v, of the oscillations due to the wave via

$$Q(z) = \sqrt{\frac{\rho_0(z) A_0(z) c_T^2(z)}{\rho_0(0) A_0(0) c_T^2(0)}} v(z). \tag{2}$$

Subscript zero denotes quantities related to the undisturbed, stationary atmosphere. ρ is the gas density, A is the cross-sectional area of the flux tube, z is the height in the atmosphere (the height scale has been chosen such that $\tau_{5000} = 1$ in the quiet sun corresponds to $z = 0$) and c_T is the tube speed defined as $c_T^2 = c_s^2 v_A^2 / (c_s^2 + v_A^2)$, where c_s is the sound speed and v_A is the Alfvén speed within the flux tube. Eq. (2) determines v once Q is known from a solution of Eq. (1).

In Eq. (1) ω is the frequency of the wave and

$$\Omega^2 = c_s^2 \left(\frac{1}{2} (\ln \gamma\zeta)'' + \frac{1}{4} \left((\ln \gamma\zeta)' \right)^2 + \frac{g}{c_s^2} \left(\left(\ln \frac{\rho_0}{p_0} \zeta \right)' + \frac{g}{c_s^2} \right) \right) - g \left((\ln \rho_0)' + \frac{g}{c_s^2} \right). \tag{3}$$

Here g is accelaration due to gravity, γ is the ratio of heat capacities, $\zeta = p_0 B_0^3 / (4\pi\gamma p_0 + B_0^2)$, p is the gas pressure and B is the magnetic field strength. Once ω and v are prescribed (the latter at two different heights in the atmosphere), Eq. (1) can be solved numerically. With the now known velocity the fluctuations to first order of the rest of the atmospheric parameters required for the calculation of line profiles can be derived from the thin tube equations in a straightforward manner.

2.2. Summary of Radiative Transfer

Since we are primarily interested in basic effects and (at the moment) not in a direct comparison with the data, we have chosen to use hypothetical lines of Fe I and II which can be selected to give an optimum coverage of line strength and excitation potential ranges with a minimum number of lines. The equivalent width W_λ and excitation potential χ_e of the chosen lines are given in Table 1. The Stokes profiles are calculated numerically. The influence of the waves is quantified by considering specific line parameters, like wavelengths, line widths, asymmetries.

The perturbations produced in the horizontal direction (due to the elasticity of the flux tube) by a longitudinal flux tube wave is observed to be small compared to the perturbations in the vertical direction. Therefore, such waves are not expected to provide a sizeable signal near the limb and cannot explain the large line widths observed there (Pantellini et al., 1988). Accordingly, the calculations presented here are restricted to solar disk centre, so that Stokes Q and U can be neglected. Therefore, in the present contribution we consider Stokes I (the unpolarised spectrum) and Stokes V (the difference between right hand circularly polarized light and left hand ciruclarly polarized light) profiles only.

3. Results

3.1. Zero-Crossing Wavelength

Figure 1 shows v_V, the zero-crossing wavelength shift of Stokes V in velocity units vs. phase of the wave for lines No. 1, 3 and 5 of Table 1. Portrayed is the influence of a propagating wave with $v(z = 0) = 1$ km s^{-1}, a wavelength of 300 km and a period of approximately 80 s. Note that the different heights of formation of the cores of the three lines are reflected by the different times or phases at which the largest redshifts for the

Table 1 Hypothetical Spectral Lines, Heights of Formation and Wave Amplitudes

Line No.	Ion	W_λ (mÅ)	χ_e (eV)	z_F (km)	$\log \tau_F$	$v_a(z_F)$ (km s^{-1})	$v_V(z_F)$ for λ_w = 900 km (km s^{-1})	$v_V(z_F)$ for λ_w = 300 km (km s^{-1})	$v_V(z_F)$ for λ_w = 150 km (km s^{-1})
1	Fe I	55	0	150	−2.2	1.3	1.15	0.8	0.25
2	Fe I	15	0	145	−2.2	1.27	1.15	0.75	0.25
3	Fe I	110	0	235	−2.75	1.5	1.55	1.3	0.3
4	Fe I	55	4	60	−1.45	1.1	1.0	0.65	0.1
5	Fe II	55	3	75	−1.6	1.13	1.05	0.8	0.35

various lines occur (arrows in Fig. 1). It should, therefore, in principle be possible to distinguish between propagating waves and standing waves or oscillations, and possibly even to deduce propagation velocities from high spatial resolution observations of purely photospheric spectral lines. Conversely, we can derive rough heights of formation from this diagram, since we know the height of the downflowing peak of the wave at a given phase.

Table 1 lists the heights of formation, z_F, and the corresponding optical depths, $\log \tau_F$, of the cores of the 5 lines, the true wave amplitudes $v_a(z_F)$ at these heights and the "wave amplitudes" derived directly from the oscillation amplitudes of the zero-crossing wavelength $v_V(z_F)$, i.e. the signal shown by simulated observations. λ_w refers to the wavelengths of the waves. All three waves have amplitudes of 1 km s^{-1} at $z = 0$. The numbers listed in these columns are the wave amplitudes as derived from the simulated observations. Although they are reasonably accurate for the wave with the longest wavelength, they can be up to 10 times too small for the λ_w = 150 km wave. This implies that the energy flux transported by flux tube waves can be underestimated by up to a factor of 100, and possibly even more for waves of even smaller λ_w, from direct observations of wavelength shifts, if no correction is made for radiative transfer effects.

There are two main reasons for the behaviour of $v_V(z_F)$ seen in Table 1. If $\lambda_w \lesssim$ the order of the width of a typical Stokes V contribution function (see Van Ballegooijen, 1985; Grossmann-Doerth et al., 1989, for definitions of the Stokes V contribution function) considerable velocity gradients occur over the width of the contribution function at certain phases, leading to the reduction of the signal in the zero-crossing wavelength. As expected this effect is seen to increase dramatically with decreasing wavelength of the wave. For Stokes I a similar effect has previously also been noticed for simple sine waves in the quiet photosphere (e.g. Keil and Marmolino, 1986).

The second effect which reduces the oscillation amplitude of the zero-crossing wavelength for a propagating tube wave (or any other propagating acoustic or magnetoacoustic wave) is the variation in temperature with phase. Whereas (in the absence of radiative damping) for standing waves the phase difference between velocity and pressure, temperature etc. is 90°, for propagating waves the phase difference is close to 180°. Therefore the temperature in the upflowing phase is lower than in the downflowing phase. As a result the temperature sensitive low excitation Fe I lines weaken considerably during the downflowing phase and strengthen during the upflowing phase, leading to a reduction of the zero-crossing oscillation amplitude and a blueshift of the line (averaged over a full oscillation period).

3.2. Line Widths

Another interesting diagnostic parameter is the line width. In time averaged observations of flux tubes strongly broadened Stokes V profiles are seen. In the past such line widths have been modelled using either macroturbulence or a mixture of macro- and microturbulence.

When the synthetic V profiles are considered as a function of time, or phase of the wave, then the widths of lines 2, 4 and 5 do not change appreciably with phase. Lines 2 and 3, on the other other hand, have larger

widths during the cool phase than during the warm phase. Measurements of line widths of well chosen lines as a function of time may, therefore, also be used to diagnose flux tube waves. Such measurements can help to overcome the ambiguities faced when attempting to derive wave amplitudes from zero-crossing shift measurements, in particular when combined with measurements of Stokes I line depth or Stokes V strength (e.g. areas of the Stokes V wings) which can also vary strongly with phase.

One interesting numerical experiment is to test the reliability of the "Gaussian micro- and macroturbulence" approximation used to describe the time averaged line broadening in flux tubes in the past (e.g. Solanki, 1986; Pantellini et al., 1988). To this end we have used isothermal propagating waves which vary purely sinusoidally with height, thus coming closest to the generally used height independent macro- or microturbulence velocity. We find that if the wavelengths of the waves are sufficiently large (e.g. much larger than the width of the Stokes V contribution function) the line widths and shapes behave qualitatively as expected from the macroturbulence approximation, i.e. the lines become broader and more "V" shaped, while waves with small wavelengths produce strongly "U" shaped lines, a clear signature of microturbulence. Also, such waves affect the width of line 3 (lying on the horizontal part of the curve of growth) more strongly than the weaker lines, also in good agreement with classical microturbulence theory. However, there are considerable quantitative differences between the effects of the waves and of the turbulence velocities, due to the generally assumed Gaussian shape for the turbulence velocity distribution which differs considerably from the distribution produced by a sinusoidal wave. This can give rise to a wrong upper limit on the mechanical flux carried by flux tube waves if the line widths are analysed using turbulence velocities.

As long as there are no temperature fluctuations, standing and propagating waves give rise to reasonably similar line broadenings. In particular, the relative broadenings of the various lines are not affected. As soon as we let the temperature vary with phase then large differences between standing and propagating waves become evident. Due to the particular phase relationship between temperature and velocity, the widths of lines formed in the presence of standing waves are not affected at all by temperature fluctuations. Widths of lines formed in the presence of propagating waves may, on the other hand, change strongly. Fig. 2 shows the line width vs. $v(0)$ for isothermal (Fig. 2a) and for moderately non-isothermal (Fig. 2b) waves (λ_w = 300 km, period of approximately 80 s). Note that lines 1 and 2 differ extremely in the two cases, being much narrower for the wave with temperature fluctuations included. The widths of these lines may even decrease somewhat again as the wave amplitude is increased. Line 3 differs only slightly and the Fe II line (No. 5) appears completely unaffected.

The observed behaviour is due to the alternate weakening and strengthening of the lines in the up- and downflowing phases, respectively. For the weak lines this implies mainly a change in line depth, while for the strong line it means mainly a change in line width. Therefore, the weak line almost disappears in the hot phase, and gives very little contribution to the average profile which thus remains quite narrow corresponding to the width of the line in the upflowing phase. For the strong line, due to its increasingly prominent wings, the increase in width during the cool phase manages to offset its decrease during the hot phase.

It is important to note that in the presence of non-isothermal waves even the line width of temperature sensitive lines can become an unreliable indicator of the wave amplitude. As seen in such lines non-isothermal short period tube waves "disappear", except for their contribution to the V asymmetry.

3.3. Stokes V Asymmetry

Finally, let us consider how the tube waves affect the Stokes V asymmetry. Firstly, standing waves, or isothermal propagating waves do not produce any net asymmetry in the Stokes V profile averaged over a full period. Non-isothermal propagating waves also produce only negligible area asymmetry δA (defined as $(A_b - A_r)/(A_b + A_r)$) in agreement with the much simpler calculations of Solanki (this volume). δa, the amplitude asymmetry defined similarly, on the other hand, can be quite substantial (of the order of 10%) in the 2-D case. Although exciting, this result is based on only a few 2-D calculations. More calculations, in particular such which consider the combination of a wave and an external downflow whose presence is

suggested by recent empirical investigations (cf. Solanki, this volume), are planned.

4. Conclusions

We have presented linear calculations of undamped magnetoacoustic waves using the thin tube approximation and have tested their influence on the Stokes I and V line parameters of a set of hypothetical spectral lines of iron. The dependence of the line parameters on waves parameters has been studied, with a view of improving the meagre observational diagnostics of flux tube waves available so far. In particular, the importance of at least linear MHD wave calculations has been demonstrated. For example, propagating magnetoacoustic waves produce an amplitude asymmetry of Stokes V, of the correct sign and approximate magnitude for a correct reproduction of the observations of some lines (cf. Solanki, these proceedings). MHD calculations are also needed to interpret line widths properly. Further calculations are underway and improvements to the description of the waves are planned.

References

Defouw, R.J., Wave Propagation Along a Magnetic Tube, *Astrophys. J.* **209**, 266–269, 1976.

Grossmann-Doerth, U., Larsson, B., and Solanki, S.K., Contribution and Response Functions for Stokes Line Profiles Formed in a Magnetic Field, *Astron. Astrophys.* **204**, 266–274, 1988.

Herbold, G., Ulmschneider, P., Spruit, H.C., and Rosner, R., Propagation of Nonlinear Radiatively Damped Longitudinal Waves Along Magnetic Fluxtubes in the Solar Atmosphere, *Astron. Astrophys.* **145**, 157, 1985.

Illing, R.M.E., Landman, D.A., and Mickey, D.L., Broad-Band Circular and Linear Polarization in Sunspots: Spectral Dependence and Theory, *Astron. Astrophys.* **41**, 183, 1975.

Keil, S.L., and Marmolino, C., , *Astrophys. J.* **310**, 912, 1986.

Musielak, Z.A., Rosner, R., and Ulmschneider, P., On the Generation of Flux Tube Waves in Stellar Convection Zones. I. Longitudinal Tube Waves Driven by External Turbulence, *Astrophys. J.* **337**, 470–484, 1989.

Pantellini, F.G.E., Solanki, S.K., and Stenflo, J.O., Velocity and Temperature in Solar Magnetic Fluxtubes from a Statistical Centre-to-Limb Analysis, *Astron. Astrophys.* **189**, 263–276, 1988.

Parker, E.N., *Cosmical Magnetic Fields*, Clarendon Press, Oxford, 1979.

Rae, I.C., and Roberts, B., Pulse Propagation in a Magnetic Flux Tube, *Astrophys. J.* **256**, 761–767, 1982.

Roberts, B., Waves in Inhomogeneous Media, in *The Hydromagnetics of the Sun*, T.D. Guyenne and J.J. Hunt (Eds.), *Proc. Fourth European Meeting on Solar Physics*, ESA SP–220, 137–145, 1984.

Roberts, B., Dynamical Processes in Magnetic Flux Tubes, in *Small Scale Magnetic Flux Concentrations in the Solar Photosphere*, W. Deinzer, M. Knölker, H.H. Voigt (Eds.), Vandenhoeck & Ruprecht, Göttingen, p. 169–190, 1986.

Roberts, B., and Webb, A.R., Vertical Motions in an Intense Magnetic Flux Tube. I, *Solar Phys.* **56**, 5–35, 1978.

Roberts, B., and Webb, A.R., Vertical Motions in an Intense Magnetic Flux Tube. III. On the Slender Flux Tube-Approximation, *Solar Phys.* **64**, 77–92, 1979.

Solanki, S.K., Velocities in Solar Magnetic Fluxtubes, *Astron. Astrophys.* **168**, 311–329, 1986.

Solanki, S.K., The Origin and the Diagnostic Capabilities of the Stokes V Asymmetry Observed in Solar Faculae and the Network, *Astron. Astrophys.* in press, 1989.

Spruit, H.C., Propagation Speeds and Acoustic Damping in Waves in Magnetic Flux Tubes, *Solar Phys.* **75**, 3–17, 1982.

Spruit, H.C., and Roberts, B., Magnetic Flux Tubes on the Sun, *Nature* **304**, 401–406, 1983.

Thomas, J.H., Hydromagnetic Waves in the Photosphere and Chromosphere, in *Theoretical Problems in High Resolution Solar Physics*, H.U. Schmidt (Ed.), Max Planck Inst. f. Astrophys., Munich, p. 126,

1985.

Van Ballegooijen, A.A., in *Measurements of Solar Vector Magnetic Fields*, M.J. Hagyard (Ed.), NASA Conf. Publ. 2374, p. 322, 1985.

Webb, A.R., and Roberts, B., Vertical Motions in an Intense Magnetic Flux Tube. V. Radiative Relaxation in a Stratified Medium, *Solar Phys.* **68**, 87–102, 1980.

Zayer, I., Solanki, S.K., and Stenflo, J.O., The Internal Magnetic Field Distribution and the Diameters of Solar Magnetic Elements, *Astron. Astrophys.* in press, 1989.

Figure captions

Fig. 1 Variation of zero-crossing wavelength shift (in km s^{-1}) of synthetic Stokes V profiles over a full period of a propagating wave with $\lambda_w = 300$ km and $v_a(0) = 1$ km s^{-1}. Squares: line 1, circles: line 3, diamonds: line 4.

Fig. 2a Line widths of all 5 lines as a function of wave amplitude at $z = 0$ for isothermal propagating waves. Squares: line 1, triangles: line 2, circles: line 3, diamonds: line 4, plusses: line 5.

Fig. 2b The same as Fig. 2a for non-isothermal waves.

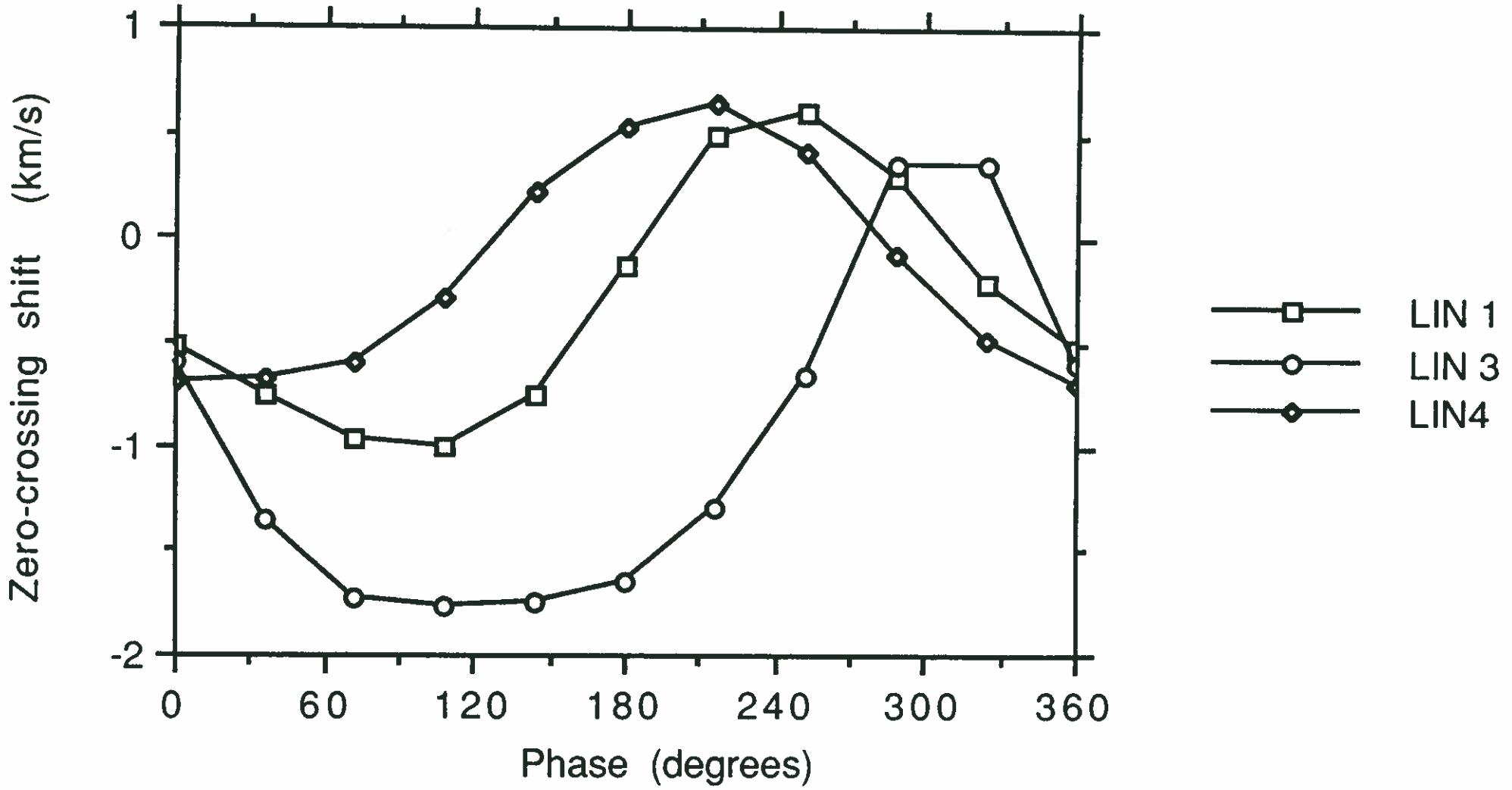
Zero-crossing shift (km/s)
1
0
-1
-2
0
60
120
180
240
300
360
Phase (degrees)
LIN 1
LIN 3
LIN4

Fig. 1

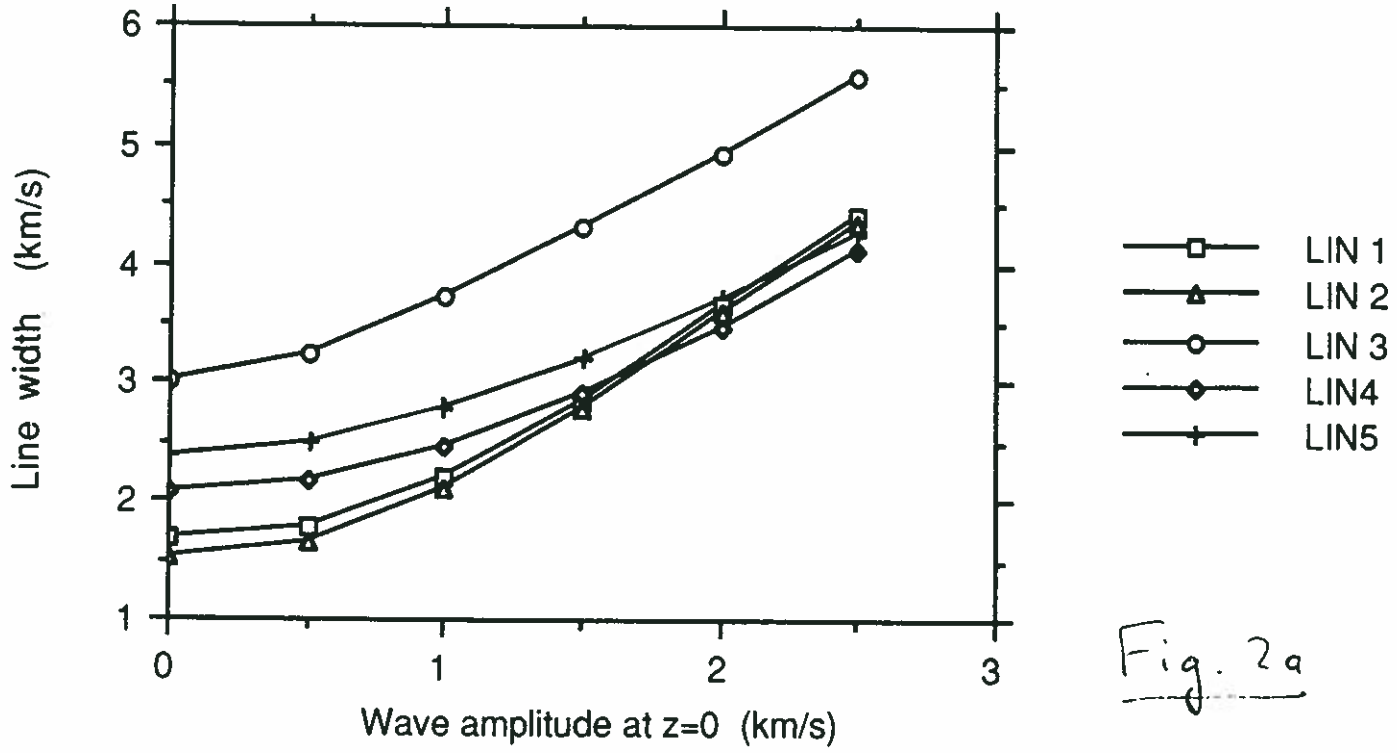
Line width (km/s)
Wave amplitude at z=0 (km/s)
0
1
2
3
1
2
3
4
5
6
LIN 1
LIN 2
LIN 3
LIN4
LIN5

Fig. 2a

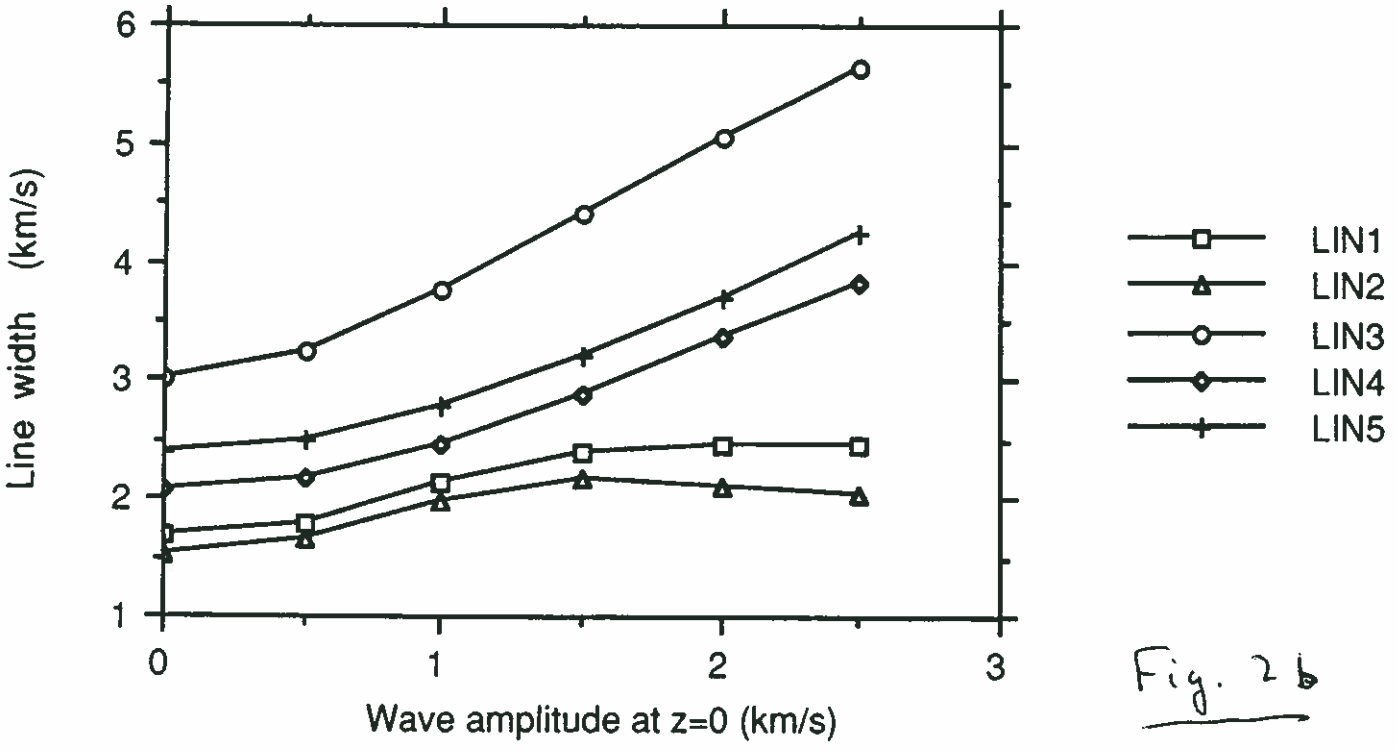
Line width (km/s)
Wave amplitude at z=0 (km/s)
0
1
2
3
1
2
3
4
5
6
LIN1
LIN2
LIN3
LIN4
LIN5

Fig. 2b